Published in final edited form as:
Toxicol Pathol. 2007 January ; 35(1): 170–177. doi:10.1080/01926230601059969.

Respiratory Tract Lesions in Noninhalation Studies

Donald M. Sells[1], **Amy E. Brix**[2], **Abraham Nyska**[3], **Micheal P. Jokinen**[4], **Denise P. Orzech**[3], and **Nigel J. Walker**[3]

[1]Battelle Columbus Laboratories, Columbus, OH 43201, USA

[2]Experimental Pathology Laboratories, Research Triangle Park, NC 27709, USA

[3]Environmental Toxicology Program, National Institute of Environmental Health Sciences, National Institute of Health, Research Triangle Park, NC 27709, USA

[4]Pathology Associates—Charles River Laboratories, Durham, NC 27703, USA

Abstract

This paper reviews respiratory tract lesions observed in rodents administered various chemicals by noninhalation routes. Chemicals administered by inhalation caused lesions in the respiratory tract and were well described; however, when chemicals were administered by noninhalation routes the effort to evaluate tissues for lesions may have been less or not considered, especially in the upper respiratory tract, and some lesions may have gone undetected. Lesions described in this review mostly occurred in rodent chronic noninhalation studies conducted by the National Toxicology Program; however, some were noted in studies of shorter duration. The nasal cavity was vulnerable to damage when chemicals were administered by noninhalation routes. Changes included respiratory epithelial hyperplasia, degeneration and necrosis of olfactory epithelium, olfactory epithelial metaplasia, adenoma, adenocarcinoma, squamous cell carcinoma, and neuroblastoma. In the lung, compound-related lesions included alveolar histiocytosis, alveolar epithelial hyperplasia, bronchiolar metaplasia of the alveolar epithelium, squamous metaplasia, alveolar/bronchial adenoma and carcinoma, and squamous tumors. Pathogenesis of these lesions included regurgitation of volatiles, metabolites arriving from the blood stream, and additional metabolism by olfactory epithelium or Clara cells. The presence of respiratory tract lesions in noninhalation studies emphasizes the need for a thorough examination of the respiratory tract including nasal passages, regardless of the route of administration.

Keywords

Toxicology; pathology; respiratory tract; rats; mice; lung; nasal epithelium

INTRODUCTION

When chemicals are administered by inhalation, intimate contact of the respiratory tract at all levels with the agent might predispose to increased respiratory tract lesions when compared to results seen when chemicals are administered by other routes. Consequently the respiratory tract is often examined more thoroughly in inhalation studies than when administration is by other routes. However, with a more thorough examination of the

Address correspondence to: Nigel Walker, National Institute of Environmental Health Sciences, National Institutes of Health, U.S. Department of Health and Human Services, 111 Alexander Drive, P.O. Box 12233, MD EC-34, Research Triangle Park, NC 27709, USA; e-mail: walker3@niehs.nih.gov.

respiratory tract (especially the nose) on a routine basis when administration was by noninhalation routes, lesions were detected with a greater frequency than was anticipated. Findings reported here were primarily observed in studies conducted for the National Toxicology Program (NTP) in rats and mice. This review was not meant to be all-inclusive, but was meant to provide examples of some lesions occurring with chemicals/drugs administered by noninhalation routes.

ANATOMY OF THE NASAL CAVITY

The nasal cavity is a complex structure within a bony case, and because of this special attention is required in preservation and sampling to obtain consistent high-quality sections for evaluation. The morphology of the nasal cavity changes considerably from anterior to posterior therefore requiring multiple sections at specific and consistent locations to properly evaluate. The nose/turbinates were not evaluated in some noninhalation studies; however, for most NTP rodent studies the nose was examined microscopically. Three levels of the nasal cavity were sectioned for NTP studies: level I, was taken immediately posterior to the upper incisor teeth; level II, was taken through the level of the incisive papilla anterior to the first palatial ridge; and level III, was taken through the middle of the second molar (Boorman et al., 1990b; Herbert et al., 1999).

At level I, the epithelium was mainly of respiratory and squamous type. A narrow band of transitional epithelium, formed of nonciliated cuboidal epithelium, bridged the transition between squamous and respiratory epithelium (Harkema, 1991). This section contained the naso- and maxillo-turbinates, the nasolacrimal duct, the tubular diverticula of the vomeronasal organ, and portions of the paired incisive ducts. Respiratory epithelium covered the nasal septum, medial aspects of the turbinates and dorsal and lateral meatuses. Keratinized squamous epithelium lined the ventral meatus and nasolacrimal ducts. If the section was taken a few millimeters posterior, olfactory epithelium might be present in the dorsal meatus.

At level II, all three types of epithelium were present. The naso- and maxillo-turbinates were still visible. The nasolacrimal ducts were lateral to the roots of the incisor teeth. The vomeronasal organ and the incisive duct, which communicates between the nasal and oral cavities, were visible. The mucosa of the dorsal meatuses and adjacent nasal septum were lined by olfactory epithelium, and the remainder of the nasal cavity was lined by respiratory epithelium with the exception of the ventral meatus, which was lined by squamous epithelium.

At level III, olfactory epithelium lined most of the cavity with the exception of small areas of respiratory epithelium on the lateral wall and some turbinates. The cavity at this level was largely filled by the ethmoid turbinates. The nasopharyngeal duct was visible at the base of the septum and olfactory lobes of the brain were visible dorsally.

NASAL LESIONS

Special attention has been given to the nose in inhalation studies where treatment-related effects were documented. As the nose became a more routine tissue for evaluation in all types of studies, nasal lesions were documented in noninhalation studies. Lesions observed in noninhalation studies were morphologically similar to those seen in inhalation studies.

Nonneoplastic Nasal Lesions

Nonneoplastic lesions included hyperplasia of respiratory epithelium; degeneration, necrosis, and atrophy of the olfactory epithelium; and metaplasia of olfactory epithelium to respiratory type with further hyperplasia of the new respiratory type epithelium.

Respiratory epithelial hyperplasia was characterized by an increase in the number of columnar cells, by formation of multiple short papillary epithelial projections, and by the formation of multiple invaginations or "crypt-like" structures (Figure 1A). The mucosa and underlying submucosa were sometimes infiltrated with polymorphonuclear and mononuclear inflammatory cells. Dilated submucosal glands, some of which were lined by hyperplastic epithelium, often accompanied the respiratory epithelial hyperplasia. Respiratory epithelial hyperplasia was observed in the respiratory epithelium lining the nasal septum, the nasal turbinates and the ventral ethmoid turbinates. Respiratory epithelial hyperplasia was diagnosed in Sprague–Dawley rats administered a binary mixture of 3,3′, 4,4′,5-pentachlorobiphenyl (PCB126) and 2,2′,4,4′,5,5′-hexachlorobiphenyl (PCB153), and a binary mixture of PCB 126 and 2,3′,4,4′,5-pentachlorobiphenyl (PCB 118) by gavage (Nyska et al., 2005).

Metaplasia of olfactory epithelium to respiratory type epithelium was noted in the olfactory epithelium lining the nasal septum, nasoturbinates, and ethmoid turbinates. Morphologically the olfactory epithelium was replaced by respiratory epithelium (Figure 1B). Metaplasia to respiratory type epithelium was sometimes followed by hyperplasia of the respiratory epithelium with the formation of papillary projections similar to that observed with hyperplasia of respiratory epithelium. Inflammation was observed in association with the olfactory epithelial metaplasia in some instances. Atrophy of the olfactory nerve cell bundles often accompanied changes in the olfactory epithelium. In the vast majority of cases respiratory metaplasia of olfactory epithelium was a sequel to olfactory degeneration/ regeneration. Modulation of normal patterns of cellular differentiation through direct actions on proliferating basal cells was suggested as a mechanism with some dioxin and dioxin-like compounds (Nyska et al., 2005). This finding was observed with a binary mixture of PCB 126 and PCB 153, and a binary mixture of PCB 126 and PCB 118, and in studies with methacrylonitrile (Nyska et al., 2003) and benzophenone, monochloracetic acid, and mercuric chloride (Table 1).

Degeneration and/or atrophy of the olfactory epithelium (Figure 1C and 1D) were characterized by a thinning and/or disorganization of the olfactory epithelial layer. Increased intercellular space and disruption of epithelium were early indicators of degeneration, which sometimes lead to vacuolization, apoptosis and necrosis. The sensory cells (bipolar neurons) were the most sensitive cells to injury in the olfactory epithelium and loss of these cells could lead to atrophy of the nerves; however, atrophy of the nerves did not occur with all chemicals that caused destruction of the olfactory epithelium (Gaskell, 1990). The damaged olfactory epithelium could repair or respiratory epithelial metaplasia could occur. Degeneration and/or atrophy was observed with methacrylonitrile (Nyska et al., 2003), benzyl acetate, dipropylene glycol, *o*-nitrotoluene, cyclohexanone oxime, butanal oxime, and methyl ethyl ketoxime (Table 1). Methacrylonitrile was metabolized by cytochrome P-450 2E1(CYP2E1) to acetone, which was eliminated along with the parent compound in the breath. CYP2E1 was increased in the lung and nasal tissues and it is possible that induction of CYP2E1 could play a role in the bioactivation of methacrylonitrile (Wang et al., 2002).

Pigmentation in the olfactory epithelium was observed with some chemicals (pentachloroanisole and trans-cinnamaldehyde) administered by the noninhalation route (Table 1). For pentachloroanisole the pigment appeared as coarse, golden brown to dark

brown intracytoplasmic granules in the olfactory epithelium, which with special stains were negative for iron and bile, and did not stain with periodic acid-Schiff. In the trans-cinnamaldehyde study the pigment was located in the basal cytoplasm of the olfactory epithelium and was characterized as a finely granular golden brown pigment consistent with lipofuscin.

A homogenous hyaline globular material, which has been diagnosed as eosinophilic globules, hyaline accumulation, or accumulation of homogenous globular hyaline material, is often observed in the respiratory and olfactory epithelium. The material ultrastructurally appeared as membrane-bound ellipsoid bodies suggestive of dilated rough endoplasmic reticulum (Popp et al., 1986). These were nonspecific entities that tended to increase with age, although they were reported to increase with treatment in some studies.

Neoplastic Nasal Lesions

Nasal tumors induced by chemicals administered by noninhalation routes included adenoma, adenocarcinoma, squamous cell carcinoma, carcinoma (not otherwise specified), and neuroblastoma (Table 1). Sex differences were observed in the incidence of tumors with some chemicals (Brown et al., 1991).

Polypoid adenoma (Figure 1E) was the most commonly induced adenoma in the nasal cavity (Brown et al., 1991), arising in the anterior nasal cavity from the respiratory epithelium of the nasoturbinates, maxilloturbinates, or lateral wall of the nasal cavity. Polypoid adenomas were sessile or pedunculated tumors formed of nonciliated cuboidal to low columnar cells that formed solid sheets or microcysts (Kerns, 1985). The nose was identified as a site of metabolic transformation of chemicals/drugs when administered by a variety of routes (Bogdanffy, 1990). Adenomas were associated with the administration of 2,3-dibromo-1-propanol, and 2,6-xylidine (Table 1). Adenocarcinomas arose from the respiratory epithelium or glandular structures. Those that arose from respiratory epithelium were exophytic or grew by lateral extension (Figure 1F). Those that arose from glandular structures formed solid sheets of round or polyhedral cells or were formed of spindle-shaped cells.

Adenocarcinomas, transitional cell carcinomas, and squamous cell carcinomas were reported to occur in the nose of Sprague–Dawley rats administered phenacetin in the diet (Isaka et al., 1979). 1,4-dinitrosopiperazine given in the drinking water caused carcinomas (adenocarcinomas, adenosquamous carcinomas and undifferentiated carcinomas) in F344 rats (Takano et al., 1982). Adenocarcinomas, squamous cell carcinomas, and adenomas and/or papillomas were reported to be increased in the nose when p-cresidine was administered in the feed to F344 rats (Reznik et al., 1981).

Squamous cell carcinomas occurred at any location in the nasal cavity. They originated from the squamous epithelium in the nasal vestibule, the ventral meatus or the nasopalatine duct, or more often they arose in areas of respiratory, transitional, or olfactory epithelium that had undergone squamous metaplasia (Herbert et al., 1999). Squamous cell carcinomas were formed of nests or cords of squamous epithelial cells with variable degrees of anaplasia and keratin formation (Figure 1G). Squamous cell carcinomas were frequently aggressive and invaded surrounding structures. Squamous cell carcinomas were attributed to administration of 1,4-dioxane (Table 1).

Tumors arising from the olfactory epithelium were quite diverse and the cell of origin difficult to determine without special techniques. A variety of names were applied to these tumors (olfactory neuroblastoma, olfactory carcinoma, esthesioblastoma, esthesioneuroepithelioma, neuroepithelial carcinoma). Because of the diverse morphologic

features that may occurred and difficulty in determining the cell of origin, the tumors were often lumped under the heading of neuroblastoma (Figure 1H) although neuroepithelial carcinoma was suggested as a term that would include tumors arising from the olfactory sensory, sustentacular cells, basal cells, or cells from Bowman's glands (Herbert et al., 1999).

Several types of olfactory neuroblastomas were described (Brown et al., 1991). One type was composed of cells with features of sustentacular cells in solid masses, with gland-like structures or rosettes being formed. A second type had features of neuronal olfactory cells. The cells were basophilic with hyperchromatic nuclei and a large nuclear to cytoplasmic ratio, and formed serpentine bands, sheets of cells, gland-like structures, and/or rosettes. A third type was characterized by confluent growths of endophytically proliferating surface epithelium that formed sheets or lobules of cells that had large nuclei with marginated chromatin and single prominent nucleoli. Neuroblastoma was diagnosed in rats administered *p*-cresidine in the diet (Table 1), and with N′-nitrosonornicotine and 4-(N-methyl-N-nitrosamino)-1-(3-pyridyl)-1-butanone given by subcutaneous injection to rats (Hecht et al., 1980).

Rhabdomyosarcomas were observed in low incidence (2/sex for the high dose group) in feed studies with 2,6-xylidine (Table 1). Because of the rarity of this tumor at this location, it was potentially treatment related. A search of the larynx and trachea found little evidence of treatment-related lesions in noninhalation studies. The larynx, however, was rarely examined in noninhalation studies.

LUNG LESIONS

The lung was routinely examined in both noninhalation and inhalation studies. A variety of lesions were associated with administration of compounds by the noninhalation route. Some included alveolar histiocytosis (macrophage infiltration of the alveoli), hyperplasia of the alveolar epithelium, bronchiolization (bronchiolar metaplasia) of the alveolar epithelium, and squamous metaplasia. Neoplastic findings included alveolar/bronchiolar adenoma and carcinoma, and squamous tumors (cystic keratinizing epithelioma, and squamous cell carcinoma).

Nonneoplastic Lung Lesions

Alveolar histiocytosis (macrophage infiltration of the alveoli) consisted of the accumulation of macrophages in alveoli (Figure 2A). These cells had abundant foamy cytoplasm and were sometimes associated with inflammation, cholesterol cleft formation, an increase in type II cells, or were present in alveoli in response to increased production of surfactants by type II cells. Alveolar histiocytosis was found in control animals but was increased in severity and incidence with the administration of some compounds. Elmiron (Nyska et al., 2002), dimethoxybenzidine dihydrochloride, and titanocene dichloride induced alveolar histiocytosis (Table 2) as well as the drugs amiodarone used for cardiac arrhythmia, ipindole used as an antidepressant, and chlorophentermine used for anorexia (Boorman et al., 1990a).

Alveolar epithelial hyperplasia (AEH) was characterized by a focal increase in type II cells lining the interalveolar septa. The cells were cuboidal and some of the septa were slightly thickened, but normal architecture was maintained (Figure 2B). AEH was associated with chronic inflammation or was a primary lesion where it was considered a precursor to alveolar/bronchiolar adenomas and carcinomas. AEH was associated with administration of *o*-nitrotoulene, riddelliine, dibromoacetic acid, *p*-nitrotoulene, 4-methylimidazole, 3,3′-dimethylbenzidine dihydrochloride, and 2,2-bis (bromomethyl)-1,3-propanediol (Table 2).

Bronchiolar metaplasia (BM) of the alveolar epithelium was characterized by metaplasia of alveolar epithelium to respiratory type primarily at the junction of the terminal bronchioles and along alveolar ducts (Figure 2C). The metaplastic cells were cuboidal to columnar, with basally located nuclei, eosinophilic cytoplasm, and cilia. Alveolar duct space and alveolar lumens often contained an amorphous, lightly basophilic to amphophilic material. Periodic Acid-Schiff and Alcian Blue staining indicated that the material was mucuslike. Scattered cells with a smooth apical surface lacking cilia, which were consistent with Clara cells, were sometimes present. These cells were distinct from those seen with alveolar epithelial hyperplasia, which had features of type II alveolar epithelial cells. BM was not associated with progression to neoplasia. In rats, this finding was associated with administration of dioxin or dioxin-like compounds such as PCB 126 and with administration *p*-nitrotoluene (Table 2). The metaplastic cells were positive for glutathione S-transferase Pi (GSTPi) staining in the PCB 126 study, similar to the staining of normal bronchiolar epithelium, suggesting specific metabolic activity of cells in the metaplastic areas (Brix et al., 2004).

Squamous lesions in the lung associated with inhalation studies were reviewed and classified by a panel of international experts (Boorman et al., 1996). Some of that spectrum of lesions was observed in noninhalation studies. Squamous metaplasia was observed in gavage studies with dioxin and dioxin-like compounds (Table 2) and was characterized by small focal areas of squamous cells in the alveolar areas. This may have represented an early stage in the progression to keratin-filled squamous lesions. These keratin-filled lesions were considered to be a family of lesions with the hallmark being the formation of large keratin-containing cysts. Pulmonary squamous metaplasia (Figure 2D) was characterized by the transition of alveolar epithelial cells to squamous metaplastic cells with distortion but not obliteration of the normal architecture. Keratin formation was evident and inflammation sometimes accompanied the change. Pulmonary keratinizing cyst was a term used to describe a more expansive lesion with distortion of the normal architecture. These keratin-filled cysts were often several centimeters in diameter.

Diagnostic features of pulmonary keratinizing cyst consisted of a cystic structure with a thin uniform wall composed of mature squamous cells that contained various amounts of keratin. Such lesions could be quite large because of the amount of keratin accumulated.

Neoplastic Lung Lesions

Cystic keratinizing epithelioma (Figure 2E) was used as a diagnosis for a benign tumor in this family of squamous lung lesions. This lesion was differentiated from a pulmonary keratinizing cyst by the nature of the wall, which was more complex, thicker, and irregular. The lesion seemed to grow by expanding into contiguous alveoli giving it a roughened irregular surface. This was in contrast to pulmonary keratinizing cysts, which had a thin uniform inner and outer wall. Additionally, mitotic figures and a lack of orderly maturation were features of cystic keratinizing epithelioma, and most lesions had a large keratin-filled cavity. Cystic keratinizing epithelioma was observed in gavage studies with dioxin and dioxin-like compounds (Table 2). Pulmonary squamous cell carcinoma was used as a diagnosis for the malignant form of the lesion. Some arose from cystic keratinizing epitheliomas where focal areas of malignancy occurred in the wall. Other carcinomas lacked keratinization. Squamous cell carcinoma was characterized by invasion of the pulmonary tissue, cellular atypia, lack of normal maturation, increased mitotic activity, and rarely metastasis (Figure 2F).

Other primary pulmonary neoplasms were classified as alveolar/bronchiolar (A/B) adenoma or carcinoma. These tumors had a solid, papillary or mixed pattern and some had areas of squamous or mucinous differentiation. Adenomas were usually distinct masses and usually caused compression of surrounding parenchyma (Figure 2G). In contrast to hyperplasia, the

normal alveolar architecture was lost. Neoplastic cells were cuboidal to round or polygonal with finely vacuolated cytoplasm. Carcinomas had a more irregular growth pattern and the neoplastic cells were more pleomorphic (Figure 2H). A/B adenomas and carcinomas were associated with the administration of a number of chemicals (Table 2) by noninhalation routes.

DISCUSSION

Exposure of the respiratory tract to chemicals can occur by two mechanisms: by inspiration or through the blood stream. Incidences of respiratory tract lesions are greater when chemicals are given by the inhalation route, and this could be explained by higher concentrations at points of contact. Sites of predilection for inhalation exposure are influenced by the physical and chemical features of the material and varying effects of air flow patterns on the material based on these physical characteristics. However, lesions also occur in the respiratory tract when materials are administered by noninhalation routes. Respiratory tissues may be exposed through the blood stream to the chemical in an unaltered state, or they may be exposed to a metabolite. Metabolism of the parent may occur in organs outside the respiratory tract such as the liver or metabolism may occur in respiratory tissues. Metabolism may detoxify a material or may result in a more toxic metabolite.

Significant enzymatic activity has been demonstrated in Bowman's glands, olfactory epithelium, and respiratory epithelium in the nose (Reed, 1993; Voigt et al., 1993). Metabolic predilection could explain regional distribution of lesions in the nasal cavity. The most commonly induced adenomas arose from the nasal or maxillary turbinates of the anterior nasal cavity or from the lateral wall of the anterior nasal cavity in poorly ciliated or transitional epithelium (Brown et al., 1991). This site has been identified as an active site for metabolism of chemicals so local metabolism could account for the predilection at these sites (Bogdanffy, 1990). In the lung, similar mechanisms of exposure exist. Cytochrome P450-dependent monooxygenases have been detected in the cytoplasm of Clara cells, ciliated cells, and type II pneumocytes and endothelial cells (Lee et al., 1995).

Additional mechanisms of exposure have been suggested, especially for the nasal tissues, to explain the occurrence of lesions in noninhalation studies. Such possibilities include regurgitation/reflux of volatiles from the stomach, inhalation of volatiles from the stomach, inhalation of volatiles from chemical-containing drinking water (Goldsworthy, et al., 1991), or by exhaling the parent or a toxic metabolite (Ghanayem et al., 1992). Otherwise noninhalation exposure may be the result of exposure through the bloodstream.

CONCLUSION

Respiratory tract lesions appeared to be more prevalent when chemicals were administered by inhalation probably because of the enhanced local concentration as compared to other modes of administration. However, with the more extensive examination of the respiratory tract (and especially the nose) in recent years in noninhalation studies, sufficient findings were noted to warrant examination routinely. Mechanisms for induction of lesions that were observed with noninhalation modes of administration included exposure of tissues through the vasculature, metabolism of chemical to a toxic metabolite in the affected organ, and exposure (nose) by exhaling a toxic metabolite. Also, inhalation of volatile materials when administered in the drinking water or from the stomach, and reflux of materials given by gavage, were suggested as mechanisms.

Acknowledgments

Thanks are expressed to Dr. Daphne Vasconcelos, Battelle Columbus, Columbus, Ohio, and Rodney Miller, Experimental Pathology Laboratories, Research Triangle Park, North Carolina, for their assistance. This paper was supported in part by the Intramural Research Program of NIEHS, NIH.

REFERENCES

Bogdanffy MS. Biotransformation enzymes in the rodent nasal mucosa: the value of a histochemical approach. Environ Health Perspect. 1990; 85:177–186. [PubMed: 2200661]

Boorman GA, Brockmann M, Carlton WW, Davis JM, Dungworth DL, Hahn FF, Mohr U, Reichhelm HB, Turusov VS, Wagner BM. Classification of cystic keratinizing squamous lesions of the rat lung: report of a workshop. Toxicol Pathol. 1996; 24:564–572. [PubMed: 8923677]

Boorman, GA.; Eustis, SL. Lung. In: Boorman, GA.; Eustis, SL.; Elwell, MR.; Montgonery, CA., Jr; MacKenzie, WF., editors. Pathology of the Fischer Rat. San Diego, CA: Academic Press; 1990a. p. 339-367.

Boorman, GA.; Morgan, KT.; Uriah, LC. Nose, larynx, and trachea. In: Boorman, GA.; Eustis, SL.; Elwell, MR.; Montgonery, CA., Jr; MacKenzie, WF., editors. Pathology of the Fischer Rat. San Diego, CA: Academic Press; 1990b. p. 315-337.

Brix AE, Jokinen MP, Walker NJ, Sells DM, Nyska A. Characterization of bronchiolar metaplasia of the alveolar epithelium in female Sprague–Dawley rats exposed to 3,3′,4,4′,5-pentachlorobiphenyl (PCB126). Toxicol Pathol. 2004; 32:333–337. [PubMed: 15204975]

Brown HR, Monticello TM, Maronpot RR, Randall HW, Hotchkiss JR, Morgan KT. Proliferative and neoplastic lesions in the rodent nasal cavity. Toxicol Pathol. 1991; 19:358–372. [PubMed: 1813982]

Gaskell BA. Nonneoplastic changes in the olfactory epithelium-experimental studies. Environ Health Perspect. 1990; 85:275–289. [PubMed: 2200667]

Ghanayem BI, Sanchez IM, Burka LT. Effects of dose, strain, and dosing vehicle on methacrylonitrile disposition in rats and identification of a novel-exhaled metabolite. Drug Metab Dispos. 1992; 20:643–652. [PubMed: 1358567]

Goldsworthy TL, Monticello TM, Morgan KT, Bermudez E, Wilson DM, Jackh R, Butterworth BE. Examination of potential mechanisms of carcinogenicity of 1,4-dioxane in rat nasal epithelial cells and hepatocytes. Arch Toxicol. 1991; 65:1–9. [PubMed: 2043044]

Harkema JR. Comparative aspects of nasal airway anatomy: relevance to inhalation toxicology. Toxicol Pathol. 1991; 19:321–336. [PubMed: 1813979]

Hecht SS, Chen CB, Ohmori T, Hoffmann D. Comparative carcinogenicity in F344 rats of the tobacco-specific nitrosamines, N′-nitrosonornicotine and 4-(N-methyl-N-nitrosamino)-1-(3-pyridyl)-1-butanone. Cancer Res. 1980; 40:298–302. [PubMed: 7356512]

Herbert, RA.; Leininger, JR. Nose, larynx, and trachea. In: Maronpot, RR.; Boorman, GA.; Gaul, BW., editors. Pathology of the Mouse. Vienna IL: Cache River Press; 1999. p. 259-292.

Isaka H, Yoshii H, Otsuji A, Koike M, Nagai Y, Koura M, Sugiyasu K, Kanabayashi T. Tumors of Sprague–Dawley rats induced by long-term feeding of phenacetin. Gann. 1979; 70:29–36. [PubMed: 446975]

Kerns, WD. Polypoid adenoma, nasal mucosa, rat. In: Jones, TC.; Mohr, U.; Hunt, RD., editors. Respiratory System, Monographs on Pathology of Laboratory Animals. Berlin: Springer-Verlag; 1985. p. 41-47.

Lee MJ, Dinsdale D. The subcellular distribution of NADPH-cytochrome P450 reductase and isoenzymes of cytochrome P450 in the lungs of rats and mice. Biochem Pharmacol. 1995; 49:1387–1394. [PubMed: 7763281]

Nyska A, Ghanayem BI. Characterization of the toxicity, mutagenicity, and carcinogenicity of methacrylonitrile in F344 Rats and B6C3F1 mice. Arch Toxicol. 2003; 77:233–242. [PubMed: 12698239]

Nyska A, Nold JB, Johnson JD, Abdo K. Lysomal-storage disorder induced by Elmiron following 90-days gavage administration in rats and mice. Toxicol Pathol. 2002; 30:178–187. [PubMed: 11950161]

Nyska A, Yoshizawa K, Jokinen MP, Brix AE, Sells DM, Wyde ME, Orzech DP, Kissling GE, Walker NJ. Olfactory epithelial metaplasia and hyperplasia in female Harlan Sprague–Dawley rats following chronic treatment with polychlorinated biphenyls. Toxicol Pathol. 2005; 33:371–377. [PubMed: 15805076]

Popp, JA.; Morgan, KT.; Everitt, J. Morphologic changes in the upper respiratory tract of rodents exposed to toxicants by inhalation. In: Roming, AD., Jr; Chambers, SF., editors. Microbeam Analysis. San Francisco, CA: San Francisco Press; 1986. p. 581-582.

Reed CJ. Drug metabolism in the nasal cavity: relevance to toxicology. Drug Metab Rev. 1993; 25:173–205. [PubMed: 8449146]

Reznik G, Reznik-Schuller HM, Hayden DW, Russfield A, Murthy AS. Morphology of nasal cavity neoplasms in F344 rats after chronic feeding of *p*-cresidine, an intermediate of dyes and pigments. Anticancer Res. 1981; 1:279–286. [PubMed: 7345971]

Takano T, Shirai T, Ogiso T, Tsuda H, Baba S, Ito N. Sequential changes in tumor development induced by 1,4-dinitrosopiperazine in the nasal cavity of F344 rats. Cancer Res. 1982; 42:4236–4240. [PubMed: 7105017]

Voigt JM, Guengerich FP, Baron J. Localization and induction of cytochrome P450 1A1 and aryl hydrocarbon hydroxylase activity in rat nasal mucosa. J Histochem Cytochem. 1993; 41:877–885. [PubMed: 8315279]

Wang H, Chanas B, Ghanayem BI. Effect of methacrylonitrile on cytochrome P-450 2E1 (CYP2E1) expression in male F344 rats. J Toxicol Environ Health A. 2002; 65:523–537. [PubMed: 11939710]

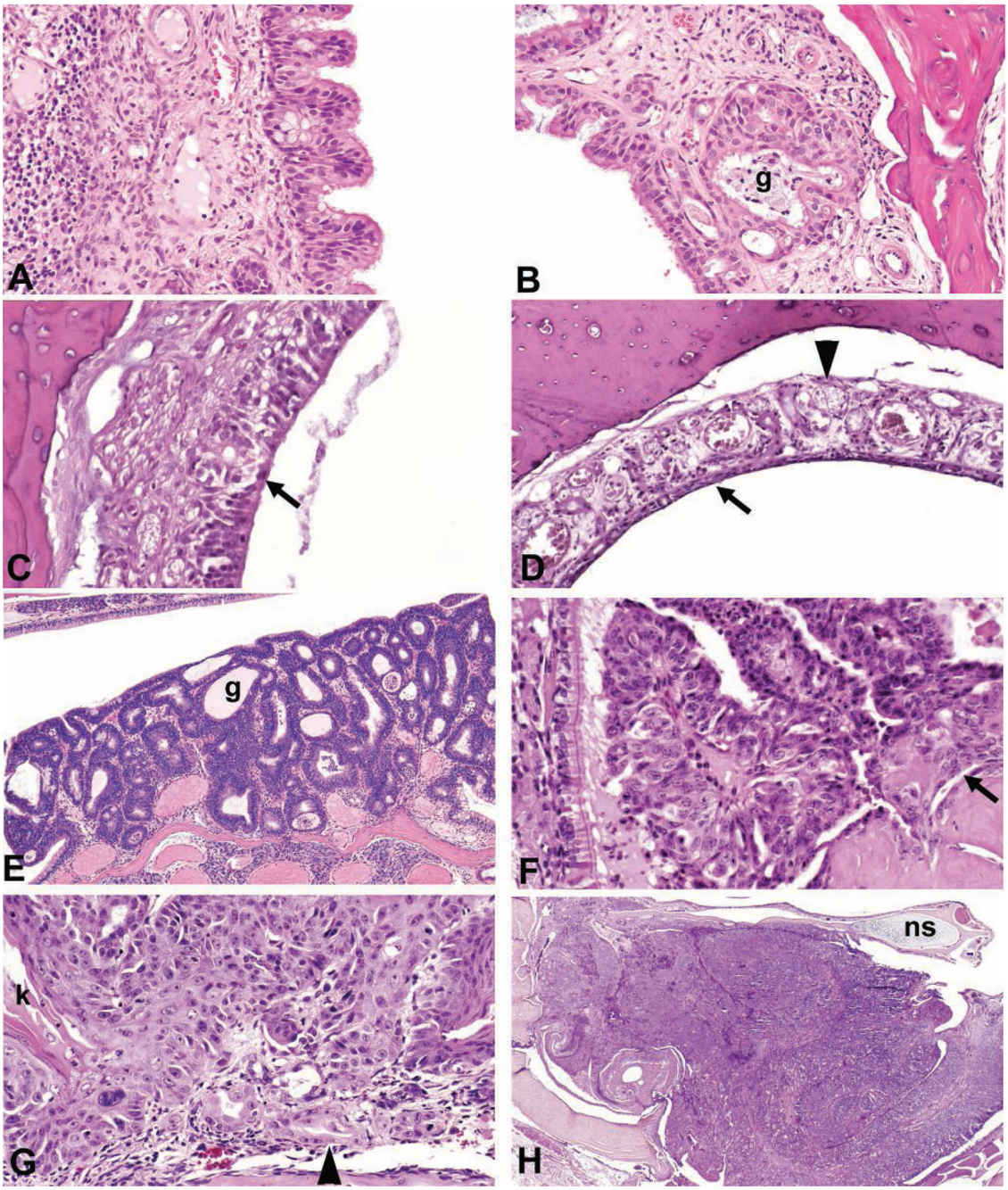

FIGURE 1.

Nose. (A) Respiratory epithelial hyperplasia in nasal septum of a rat with the formation of multiple short papillary epithelial projections and infiltration of inflammatory cells in the lamina propria. (B) Respiratory epithelial metaplasia in the dorsal meatus of a mouse with the formation of multiple short papillary epithelial projections, and dilatation and hyperplasia of Bowman's glands (g). (C) Olfactory epithelial degeneration in the dorsal meatus of a rat with disorganization and vacuolization (arrow) of the olfactory epithelial layer. (D) Olfactory epithelial atrophy/thinning (arrow) in the dorsal meatus of a rat with atrophy of the olfactory nerves (arrow head). (E) Adenoma in a rat nose formed of cuboidal to columnar epithelial cells with gland-like (g) structures. (F) Adenocarcinoma in a mouse

nose arising from respiratory epithelium with papillary formations and invasion (arrow) of lamina propria. (G) Squamous cell carcinoma in a rat nose with the formation of nests and cords of squamous cells, anaplasia, keratin formation (k) and invasion (arrow head) of lamina propria. (H) Neuroblastoma filling one side of the nasal cavity of a rat. Nasal septum (ns) at top. All sections were stained with hematoxylin and eosin.

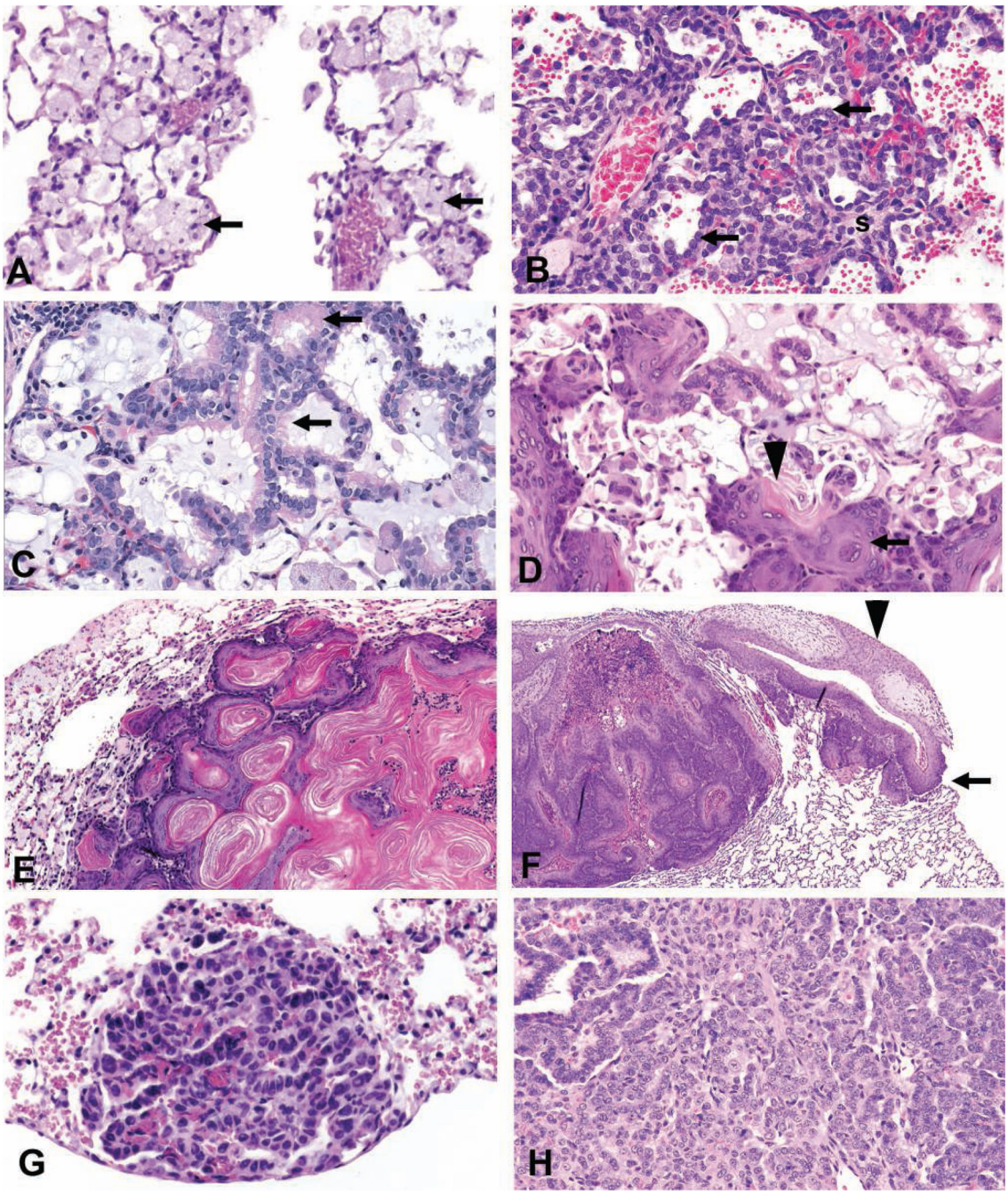

FIGURE 2.

Lung. (A) Alveolar histiocytosis in a rat characterized by the accumulation of macrophages (arrows) with abundant foamy cytoplasm in alveoli. (B) Alveolar epithelial hyperplasia in a rat characterized by an increase in cuboidal type II cells (arrows) lining interalveolar septa (s) which are thickened. (C) Bronchiolar metaplasia of alveolar epithelium in a rat where alveolar type I cells are replaced by columnar ciliated cells (arrows). The alveolar lumen contains a basophilic mucin-like material. (D) Squamous metaplasia in a rat lung characterized by the metaplasia of alveolar epithelial cells to squamous cells (arrow), distortion but not obliteration of the normal architecture, and keratin (arrowhead) formation. (E) Benign cystic keratinizing epithelioma in a rat lung characterized by a complex, thick

irregular wall, expansive growth into contiguous alveoli, lack of orderly maturation, and the formation of a large keratin-filled cavity. (F) Squamous cell carcinoma in a rat lung characterized by extension through the pleura (arrow) and scirrhous reaction (arrowhead). (G) A/B adenoma in a mouse lung consisting of cuboidal to polygonal cells in a papillary pattern with a distinct border and mild compression. (H) A/B carcinoma in a mouse lung consisting of anaplastic cells with a heterogeneous growth pattern. All sections were stained with hematoxylin and eosin.

TABLE 1

Chemical-induced nasal lesions in noninhalation NTP studies.

Diagnosis	Chemical	Route[a]	Species	Sex	TR No.[b]
Hyperplasia, Respiratory Epithelium	Binary Mixture, PCB 126 & PCB 153	G	Rat	F[c]	530
Hyperplasia, Respiratory Epithelium	Binary Mixture, PCB 126 & PCB 118	G	Rat	F[c]	531
Metaplasia, Olfactory Epithelium	Binary Mixture, PCB 126 & PCB 153	G	Rat	F[c]	530
Metaplasia, Olfactory Epithelium	Binary Mixture, PCB 126 & PCB 118	G	Rat	F[c]	531
Metaplasia, Olfactory Epithelium	Benzophenone	F	Mice	M&F	533
Metaplasia, Olfactory Epithelium	Monochloroacetic Acid	G	Mice	M&F	396
Metaplasia, Olfactory Epithelium	Mercuric Chloride	G	Mice	M&F	408
Epithelial Dysplasia, Nasal Cavity	2,3-Dibromo-1-Propanol	D	Rat	M&F	400
Atrophy/Metaplasia, Olfactory Epithelium	Methacrylonitrile	G	Rat	M&F	497
Atrophy, Olfactory Epithelium	Dipropylene Glycol	DW	Rat	M	511
Atrophy/Degeneration, Olfactory Epithelium	Benzyl Acetate	F	Mice	M&F	431
Cystic Hyperplasia, Glands	Benzyl Acetate	F	Mice	M&F	431
Degeneration, Olfactory Epithelium	Dipropylene Glycol	DW	Rat	M&F	511
Degeneration, Olfactory Epithelium	*o*-Nitrotoluene	F	Mice	M&F	504
Degeneration, Olfactory Epithelium	Cyclohexanone Oxime	DW	Mice	M&F	50
Degeneration, Olfactory Epithelium	Butanal Oxime	DW	Mice & Rat	M&F	69
Degeneration, Olfactory Epithelium	Methyl Ethyl Ketoxime	DW	Rat	M&F	51
Cystic Hyperplasia, Submucosal Glands	Benzyl Acetate	F	Mice	M&F	431
Pigmentation, Olfactory Epithelium	Pentachloroanisole	G	Rat	M&F	414
Pigmentation, Olfactory Epithelium	trans-Cinnamaldehyde	F	Mice	M&F	514
Adenoma	2,3-Dibromo-1-Propanol	D	Rat	M&F	400
Adenoma	2,3-Dibromo-1-Propanol	D	Mice	M	400
Adenoma/Carcinoma	2,6-Xylidine	F	Rat	M&F	278
Carcinoma	Pentachlorophenol	F	Rat	M[d]	483
Squamous Cell Carcinoma	1,4-Dioxane	DW	Rat	M&F	80
Carcinoma, NOS	Dimethylvinyl Chloride	G	Rat	MF	316
Neuroblastoma	*p*-Cresidine	F	Rat	M&F	142

Diagnosis	Chemical	Route[a]	Species	Sex	TR No.[b]
Rhabdomyosarcoma	2,6-Xylidine	F	Rat	M&F[d]	278

TCDD = 2,3,7,8-Tetrachlorodibenzo-*p*-dioxin; PeCDF = 2,3,4,7,8-Pentachlorodibenzofuran; PCB 118 = 2,3′,4,4′,5-Pentachlorobiphenyl; PCB 126 = 3,3′,4,4′,5-Pentachlorobiphenyl; PCB 153 = 2,2′,4,4′,5,5′,-Hexachlorobiphenyl.

[a] D: dermal, F: feed., DW: drinking water, G: gavage.

[b] TR No.: technical report number (can be accessed at: ⟨http://ntp.niehs.nih.gov.go/14374⟩).

[c] Only female rats used in the study.

[d] May have been related/equivocal, two high-dose rats affected in each sex.

TABLE 2

Chemical-induced lung lesions in noninhalation NTP studies.

Diagnosis	Chemical	Route[a]	Species	Sex	TR No.[b]
Infiltration Cellular, Histiocytic	Elmiron	G	Rat	M&F	512
Infiltration Cellular, Histiocytic	Dimethoxybenzidine Dihydrochloride	DW	Rat	M&F	372
Infiltration Cellular, Histiocytic	Titanocene Dichloride	G	Rat	M&F	399
Hyperplasia, Alveolar Epithelium	*o*-Nitrotoluene	F	Rat	M&F	504
Hyperplasia, Alveolar Epithelium	Riddelliine	G	Mice	F	508
Hyperplasia, Alveolar Epithelium	Dibromoacetic Acid	DW	Rat	F	537
Hyperplasia, Alveolar Epithelium	*p*-Nitrotoluene	F	Mice	M	498
Hyperplasia, Alveolar Epithelium	4-Methylimidazole	F	Mice	F	535
Hyperplasia, Alveolar Epithelium	3,3′-Dimethylbenzidine dihydrochloride	DW	Rat	M&F	390
Hyperplasia, Alveolar Epithelium	2,2-Bis (Bromomethyl)-1,3-Propanediol	F	Mice	F	452
Alveolar/Bronchiolar Hyperplasia	2,2-Bis (Bromomethyl)-1,3-Propanediol	F	Rat	M	452
Bronchial Epithelial Pleomorphism, Focal Hyperplasia	2,3-Dibromo-1-Propanol	D	Mice	M&F	400
Hyperplasia, Bronchial Epithelium	Benzofuran	G	Mice	M&F	370
Bronchiolization, Alveolar Epithelium	*p*-Nitrotoulene	F	Mice	M&F	498
Metaplasia, Alveolar Epithelium	Tetrachlorodibenzo-*p*-dioxin	G	Rat	F[c]	521
Metaplasia, Alveolar Epithelium	2,3,4,7,8-Pentachlorodibenzofuran	G	Rat	F[c]	525
Alveolar Epithelium, Metaplasia, Bronchiolar	Binary Mixture, PCB 126 & PCB 153	G	Rat	F[c]	530
Alveolar Epithelium, Metaplasia, Bronchiolar	Mixture, TCDD, PeCDF, & PCB 126	G	Rat	F[c]	526
Alveolar Epithelium, Metaplasia, Bronchiolar	Binary Mixture, PCB 126 & PCB 118	G	Rat	F[c]	531
Alveolar Epithelium, Metaplasia, Bronchiolar	PCB 126	G	Rat	F[c]	520
Squamous Metaplasia	Mixture, TCDD, PeCDF, PCB 126	G	Rat	F[c]	526
Squamous Metaplasia	Binary Mixture, PCB 126 & PCB 118	G	Rat	F[c]	531
Squamous Metaplasia	Binary Mixture, PCB 126 & PCB 153	G	Rat	F[c]	530
Squamous Metaplasia	PCB 126	G	Rat	F[c]	520
Squamous Metaplasia	2,3,4,7,8-Pentachlorodibenzofuran	G	Rat	F[c]	525

Diagnosis	Chemical	Route[a]	Species	Sex	TR No.[b]
Adenoma	Oxymetholone	G	Rat	F	485
A/B Adenoma	1-Amino-2-4-dibromoanthraquinone	F	Mice	M&F	383
A/B Adenoma	3,3′-Dimethylbenzidine dihydrochloride	DW	Rat	M&F	390
A/B Adenoma	1,2-Dichloroethane	G	Mice	M&F	55
A/B Adenoma	Dibromoacetic Acid	DW	Mice	M	537
A/B Adenoma/Carcinoma	Riddelliine	G	Mice	F	508
A/B Adenoma/Carcinoma	*o*-Nitrotoluene	F	Rat	F	504
A/B Adenoma/Carcinoma	*p*-Nitrotoluene	F	Mice	M[d]	498
A/B Adenoma/Carcinoma	4-Methylimidazole	F	Mice	M&F	535
A/B Adenoma/Carcinoma	n-Methylolacrylamide	G	Mice	M&F	352
A/B Adenoma/Carcinoma	2,2-Bis (Bromomethyl)-1,3-Propanediol	F	Mice	M&F	452
A/B Adenoma/Carcinoma	Benzofuran	G	Mice	M&F	370
Cystic Keratinizing Epithelioma	Tetrachlorodibenzo-*p*-dioxin	G	Rat	F[c]	521
Cystic Keratinizing Epithelioma	Binary Mixture, PCB 126 & PCB 153	G	Rat	F[c]	530
Cystic Keratinizing Epithelioma	Binary Mixture, PCB 126 & PCB 118	G	Rat	F[c]	531
Cystic Keratinizing Epithelioma	Mixture, TCDD, PeCDF, PCB 126	G	Rat	F[c]	526
Cystic Keratinizing Epithelioma	PCB 126	G	Rat	F[c]	520
Squamous Cell Carcinoma	PCB 126	G	Rat	F[c]	520

TCDD = 2,3,7,8-Tetrachlorodibenzo-*p*-dioxin; PeCDF = 2,3,4,7,8-Pentachlorodibenzofuran; PCB 118 = 2,3′,4,4′,5-Pentachlorobiphenyl; PCB 126 = 3,3′,4,4′,5-Pentachlorobiphenyl; PCB 153 = 2,2′,4,4′,5,5′,-Hexachlorobiphenyl.

[a] D: dermal, F: feed, DW: drinking water, G: gavage.

[b] TR No.: technical report number (can be accessed at: ⟨http://ntp.niehs.nih.gov.go/14374⟩).

[c] Only female rats used in the study.

[d] May have been related/equivocal, two high-dose rats affected in each sex.